Parametric study on push-up loading of sand plug in open-ended pipe pile using DEM

Parametric study on push-up loading of sand plug in open-ended pipe pile using DEM

T. Shintani, T. Matsumoto, P. Kitiyodom & H. Kawano
Graduate School of Natural Science and Technology, Kanazawa University, Japan

K. Haneda
Department of Civil Engineering, Kanazawa University, Japan

ABSTRACT: The bearing capacity of an open-ended pipe pile consists of outer shaft resistance, toe resistance and soil plug resistance (inner shaft resistance). The soil plug capacity is thought to be largely controlled by height and stress states of soil plug that is formed inside the pile during installation process. However, these aspects have not been fully clarified. In this paper, parametric study on push-up loading of soil plug was carried out using three-dimensional discrete element method for the first step to investigate the bearing mechanism of open-ended pipe pile. Influence of dilatancy of sand and the soil plug height was focused.

1 INTRODUCTION

The bearing capacity of an open-ended pipe pile is composed of outer shaft resistance, toe resistance and inner shaft resistance (soil plug capacity). It is thought that the soil plug capacity is largely controlled by height and the stress states of soil plug that is formed inside the pile during installation process. Theoretical, numerical and experimental works on plugging or push-up loading of soil plug have been done by many researchers, as Matsumoto et al (2004) summarised.

For examples, a theoretical approach to estimate the plug capacity was presented by Yamahara (1964a, b). Kitiyodom et al (2005) have carried out a series of dynamic and static load tests on model open-ended pipe piles in dry dense silica sand, in order to investigate influence of pile installation method, coefficient of friction between the sand and the inner shaft on the soil plug capacity.

However, mechanisms of formation of soil plug and its capacity have not been fully clarified, because the soils surrounding and inside the pipe pile undergo very large deformations and failures during pile installation process.

In this paper, parametric study on push-up loading of soil plugs are carried out using 3D-DEM for the first step to investigate the bearing mechanism of open-ended pipe piles, although push-up load test of soil plug was not performed in the pile load tests by Kitiyodom et al (2005).

First, 3D-DEM analyses of the maximum and minimum density tests, one-dimensional compression and direct shear tests of the model ground sand were performed, in order to determine analysis parameters such as particle shape and spring stiffness between the particles. Then, parametric study on push-up loading of soil plugs was carried out using the determined analysis parameters. Influence of dilatancy of dense and loose sands, and the height of soil plug was focused in the parametric study.

2 ELEMENT TESTS

2.1 *Outline of element tests performed*

The sand used in the model pile load tests was a silica sand having relatively uniform particle sizes as shown in Table 1. The physical properties of the sand are summarised in Table 1. Note that the model ground was highly compacted to have relative density, D_r, greater than 90 %.

One-dimensional compression tests of the sand were carried out using the oedometer test device, and direct shear tests were carried out with different vertical stresses. Furthermore, maximum density test and minimum density test were carried out.

In this chapter, the above-mentioned element tests are analysed using 3D-DEM to determine analysis parameters, such as particle shape and size, spring stiffness and coefficient of friction between particles, and density of particles, appropriately.

Table 1. Physical properties of the silica sand.

Property	Value
Relative density at test, D_r	> 90 %
Density of soil particle , ρ_s	2.68 t/m^3
Maximum density, ρ_{max}	1.690 t/m^3
Minimum density, ρ_{min}	1.389 t/m^3
Maximum void ratio, e_{max}	0.927
Minimum void ratio, e_{min}	0.583
Mean grain size, D_{50}	0.126 mm
Coefficient of uniformity, U_c	2.268

2.2 *Analysis conditions*

The DEM code used in this study was PFC3D (Itasca, 2003). 'Clump' that is shown in Figure 1 was employed in the DEM analyses. A clump is composed of spheres that are overlapping partly to form a non-spherical particle. In this parametric study, the sand was modelled by peanut-shaped clumps composing of two spheres as shown in Figure 1, following Katzenbach & Schmitt (2004).

It is desirable to use the same particle size as the real sand in DEM simulation. However, such modelling is practically impossible, in view of capacity and time of calculation. In centrifuge tests, no scale effect was observed for model footings that had ratios of footing diameter to soil particle size ranging from 30 to 180 (Ovesen, 1979).

Diameter of the soil plug in parametric calculation in this paper is about 100 mm. According to the above observation in centrifuge tests, the particle size used in DEM should be less than 3 mm. However, the use of clumps consisting of 2 spheres having a diameter of 3 mm took a very long calculation time. Hence, the authors decided to use peanut-shaped clumps having a diameter of 4 mm as shown in Figure 1.

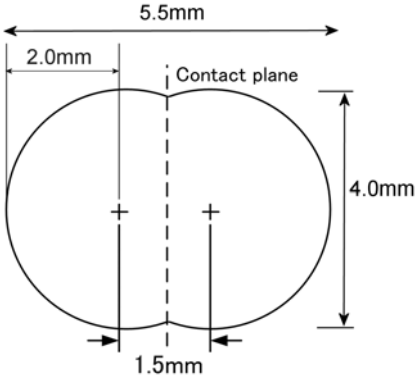

Figure 1. Peanut-shaped clump used in the DEM analyses.

The values of normal spring, tangential spring and the friction coefficient between the clumps were determined through matching analyses of the element tests (results are shown later). The identified analysis parameters are summarised in Table 2. Note that local damping value (Itasca 2003) of 0.7 was employed and any other damping was not used through the analyses. Calculation timestep used was 5 μs for all the DEM analyses except for the analysis of direct shear test where timestep of 2 μs was used.

Table 2. Analysis parameters of clump.

Property	Value
Particle size (Long axis)	5.5 mm
(Short axis)	4.0 mm
Density of soil particles, ρ_s ! !	2.73 t/m^3
Friction angle between clumps, ϕ_μ	35 degrees
Normal and tangential spring stiffness between clumps	5Ø 10^5 N/m
Normal and tangential spring stiffness between clump and wall	5Ø 10^5 N/m

2.3 *Maximum density and Minimum density tests*

Maximum density and minimum density tests were carried out. The minimum density test followed the standard method by Japanese Geotechnical Society (1992). On the other hand, non-standard method was used in the maximum density test. In the standard method, the sand is poured into the mould (40 mm high) with a collar (20 mm high) in 10 layers, and 100 impacts are applied to the mould after pouring each soil layer. In non-standard method used in this research, the sand was poured into the mould with the collar at once, and 1000 impacts were applied to the mould, as shown in Figure 2.

Figure 2 shows the analytical models for the minimum and maximum density tests. The hopper, mould and collar were modelled by 'wall elements'. A total of five DEM analyses of minimum and maximum density tests were carried out.

Clumps were created every time randomly inside the hopper (Fig. 2(a)). Afterwards, the hopper was pulled-up at a speed of 5 mm/s. After the clumps had dropped into the mould with collar (Fig. 2(b)), the clumps in the collar were deleted (Fig. 2(c)) to obtain the maximum void ratio, e_{max}.

DEM analysis of the maximum density test was started from the state of Figure 2(b). In order to model the impact on the mould, sinusoidal horizontal displacement having a frequency of 5 Hz and an amplitude of 5 mm was applied to the mould. The shaking direction was changed by 36 degrees every 10 cycles of shaking, to simulate the test procedure.

The results of DEM analyses of the minimum density tests are summarised in Table 3. The mean values of maximum void ratio and minimum dry density are 0.958 and 1.397 ton/m^3, respectively. These values may be comparable with those obtained from the minimum density test (see Table 1).

The results of DEM analyses of the maximum density tests are compared with the test results in Figure 3.

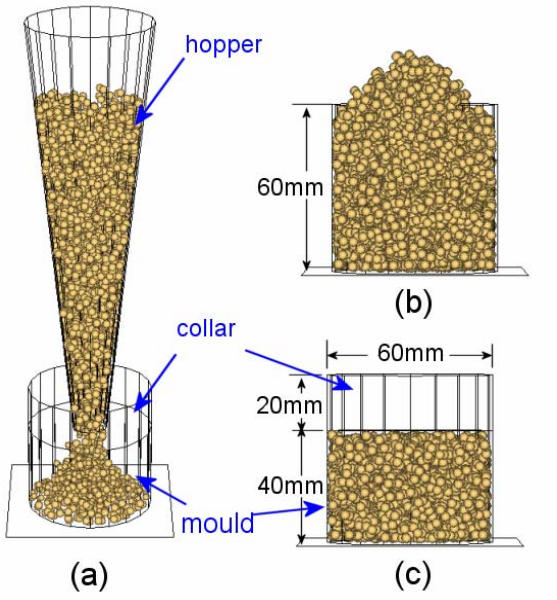

Figure 2. Analysis models used for minimum density test and maximum density test.

Table 3. The calculated results of minimum density tests

Analysis	Maximum void ratio	Minimum dry density
1st	0.976	1.384 t/m^3
2nd	0.946	1.405 t/m^3
3rd	0.944	1.406 t/m^3
4th	0.962	1.394 t/m^3
5th	0.960	1.395 t/m^3
Mean	0.958	1.397 t/m^3

Table 4. The calculated results of maximum density tests

Analysis	Minimum void ratio	Maximum dry density
1st	0.678	1.629 t/m^3
2nd	0.672	1.635 t/m^3
3rd	0.682	1.625 t/m^3
4th	0.671	1.636 t/m^3
5th	0.676	1.631 t/m^3
Mean	0.676	1.631 t/m^3

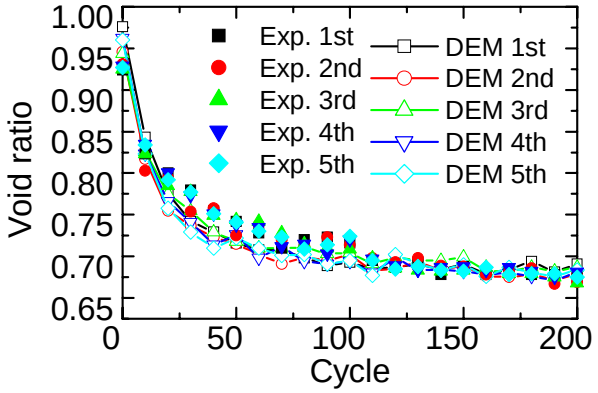

Figure 3. The calculated and experimental results of maximum density tests until 200 shaking cycles.

Changes in void ratio are plotted against the number of shaking cycles in Figure 3 until the shaking cycle of 200, although 1000 shaking cycles were analysed. The void ratio rapidly decreased with increasing shaking cycle to about 100 cycles and then almost levelled off for further shaking cycles in the non-standard maximum density tests. The results of DEM analyses simulate this measured behaviour well. The minimum void ratio and the corresponding maximum dry density obtained from the DEM analyses are summarised in Table 4.

2.4 *One-dimensional compression test*

The one-dimensional compression tests and the direct shear tests of the sand were carried out using the consolidation ring and the shear ring having an inner diameter of 60 mm and a height of 20 mm. However, in the DEM analyses, the height of the soil specimen was set at 40 mm in the DEM analyses, because the size of clump (Figure 1) seemed to be large compared to the actual ring height of 20 mm.

The friction between the clumps and the walls was neglected. The initial void ratio prior to compression was set at 0.693 in the DEM analysis. In the process of DEM analysis of the one-dimensional compression test, a total of 8 loading steps, 9.8 to 1254.4 kPa, were applied to the top loading plate.

Figure 4 shows the comparison between the one-dimensional test results and the DEM analysis results. It can be seen from the figure that the test results are well simulated by the DEM analysis.

Another results of DEM analysis of one-dimensional compression test of the dense sand are shown in Figure 5. The change in the horizontal stress, σ_h, acting on the sidewall of the ring is plotted against the vertical stress, σ_v. The value of the coefficient of earth pressure at rest, $K_0 = \sigma_h/\sigma_v$, was calculated and is plotted against the vertical stress, σ_v, in Figure 5.

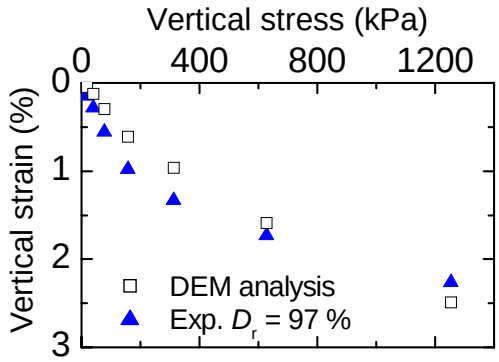

Figure 4. The calculated and experimental results of one-dimensional compression test.

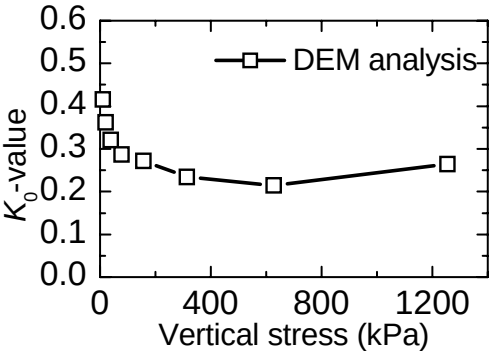

Figure 5. Vertical stress versus K_0-value.

2.5 *Direct shear test*

Direct shear test was carried out with a vertical stress of 78.4 kPa for the dense sand having D_r = 93 % (e = 0.608). In the DEM analysis, the initial void ratio prior to compression was set at 0.693 and vertical stress of 78.4 kPa was applied to the specimen through the top loading plate. After completion of the analysis of the vertical loading, horizontal displacement was applied to the upper ring at a displacement rate of 0.4 mm/min.

Figure 6 shows the comparison between the results of the direct shear test and the DEM analysis. Figure 6(a) shows the relationships between the shear displacement and the shear stress. Figure 6(b) shows the relationships between the shear displacement and the vertical strain. It can be seen from Figure 6(a) that the experimental result was simulated well by the DEM analysis and that ϕ_{peak} value is estimated as 49

degrees that is larger than the grain-to-grain friction angle, ϕ_μ, of 35 degrees. The dilatancy behaviour observed in the experiment was also simulated well by the DEM analysis (Fig. 6(b)).

It may be interesting to note that K_0-value from the well-known Jaky's equation, $K_0 = 1 - \sin \phi$, with $\phi = 49$ degrees results in $K_0 = 0.245$. This value is obtained from the DEM analysis of the one-dimensional compression test as shown in Figure 5.

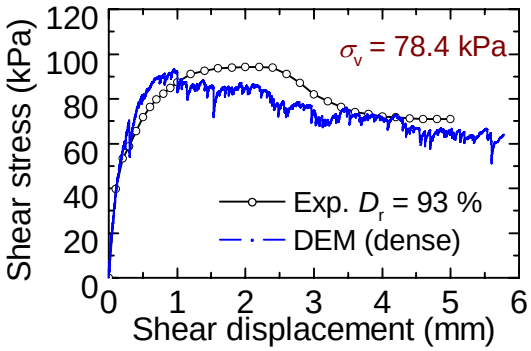

(a) Shear displacement vs shear stress

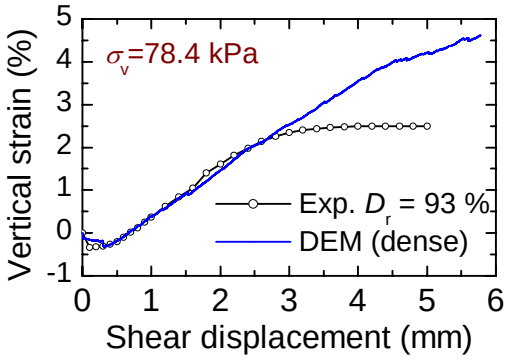

(b) Shear displacement vs vertical strain

Figure 6. The calculated and experimental results of direct shear test.

2.6 *Analytical conditions of loose sand*

In the parametric study of push-up loading of soil plug in the next chapter, influence of dilatancy behaviour of the soil on the soil plug capacity will be considered. Therefore, fictitious loose sand was created by DEM as follows for comparison with the dense sand. The loose sand was modelled by spherical particles having a uniform diameter of 4 mm. Other parameters are listed in Table 5.

Figure 7 shows the results of DEM simulation of the direct shear test with vertical stress of 78.4 kPa. Void ratio prior to vertical loading was set at 0.815 (D_r = 18.5 %). It can be seen from Figure 7 that the results of the DEM simulation exhibit a typical behaviour of loose sand, compared with the dense sand (Figure 6) and the experimental results of a medium sand that are shown in Figure 7.

Through the DEM analyses of the various element tests mentioned above, DEM analysis parameters for the dense sand are determined appropriately. These analysis parameters are used for parametric study of push-up loading on soil plug in the next chapter.

Table 5. Properties of spherical particle.

Property	Value
Particle size	4.0 mm
Density of soil particle ρ_s !	2.65 t/m^3
Friction angle between particles, ϕ_μ	35 degrees
Spring stiffness between soil particles	5Ø 10^5 N/m

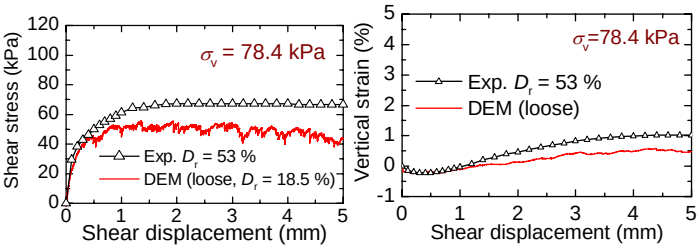

(a) Shear displacement vs shear stress

(b) Shear displacement vs vertical strain

Figure 7. The calculated and experimental results of direct shear test.

3 SIMULATION OF PUSH-UP LOADING OF SOIL PLUG

3.1 *Simulation procedure*

Although push-up load test of soil plug was not conducted, parametric study of push-up loading of soil plug are conducted in this section, in order to investigate the factors influencing the soil plugging.

Figure 8 shows the analysis model of push-up loading of soil plug. Considering axi-symmetrical condition of the problem, only one-fourth of the pile and the soil plug were modelled. The pile was modelled by rigid walls. Hence the deformation of the pile body was not taken into account in the analysis. The property of the model pile is summarised in Table 6. The pile was 100 mm in inner diameter and 0.8 m in length. The friction coefficient between the model pile and the clump was assumed as 0.44.

The soil particles (clumps or spheres) were generated inside the model pile in order to create the soil plug. Then, self-weight analysis was conducted without friction between the soil and the inner pile shaft. Finally, the simulation of push-up loading was carried out by applying an upward velocity of 5 mm/s to the rigid loading plate, taking into account the friction between the soil and the inner pile shaft. The aspect ratio of the soil plug height, H, to the inner pile diameter, D, was varied from 3 to 6.

Two series of parametric simulations were carried out for the dense sand and the loose sand. For the dense sand, the soil plug was modelled by the clumps (Figure 1). The void ratio of the soil plug in each simulation for the dense sand is shown in Table 7. These void ratios are almost equal to that (e = 0.693) used in the DEM analysis of direct shear test (see Fig 6). For the loose sand, the soil plug was modelled by the spheres (see Table 8).

Table 6. Properties of the model pile.

Property	Value
Length, L	800 mm
Inner diameter, D	100 mm
Coefficient of friction between the soil particles and wall, μ	0.44

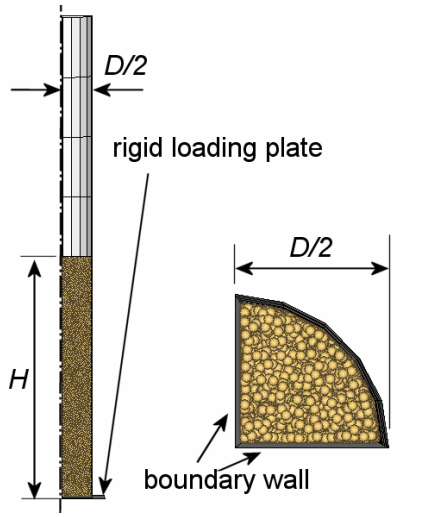

Figure 8. Analysis model of push-up load test of soil plug.

Table 7. Properties of the dense soil plug (clump).

H/D	3	4	5	6
Height, H	0.3 m	0.4 m	0.5 m	0.6 m
Void ratio, e	0.713	0.708	0.700	0.706
Dry density of soil plug, ρ_d	1.60 t/m^3	1.60 t/m^3	1.61 t/m^3	1.60 t/m^3

Table 8. Properties of the loose soil plug (sphere).

H/D	3	4	5	6
Height ,H	0.3 m	0.4 m	0.5 m	0.6 m
Void ratio, e	0.812	0.813	0.812	0.813
Dry density of soil plug, ρ_d	1.46 t/m^3	1.46 t/m^3	1.46 t/m^3	1.46 t/m^3

3.2 *Simulation results*

Figure 9 shows the relationships between the push-up displacement of the loading plate and the push-up force. Note that the push-up force in Figure 9 is 4 times the calculated value, because one-forth of the pile and the soil plug was modelled in the DEM analysis. The peak push-up force increases with increasing H/D in both sands, although the push-up force at a given push-up displacement is much higher in the dense sand. Softening behaviour occurs even for H/D = 6 in the loose sand, while softening can be seen for only H/D = 3 in the dense sand.

Let us see here the results of the DEM simulations for the cases of H/D = 4 in detail.

Figures 10(a) and 11(a) show the distributions of radial stresses and shear stresses acting along the inner pile shaft, respectively, at each push-up force for the dense sand. Figures 10(b) and 11(b) show those for the loose sand. Radial and shear stresses were calculated from the vertical force and the radial force acting on each pile wall divided by its area.

As the radial stress becomes larger, the shear stress becomes larger. Hence the push-up becomes larger. For the dense sand, the ratio of the shear stress and the radial stress ranges from 0.35 to 0.40 that is a little bit of smaller than the prescribed value of the coefficient of friction between the soil and the pile of 0.44. In contrast for the loose sand, the ratio of the shear stress and the radial stress ranges from 0.22 to 0.34 that is lower than the values for the dense sand.

It may be inferred from this result that rotation of the soil particles adjacent to the pile shaft, rather than slippage between the soil particles and the pile shaft, controls the inner shaft resistance. Further study is needed to clarify this aspect.

3.3 *Comparisons with Yamahara's equation*

Yamahara (1964a, b) presented a theoretical equation (1) to give the maximum push-up force of the soil plug. In this theory, the soil plug is assumed to be a rigid body, and equation (1) is based on the force equilibrium of a thin soil plug element.

$$p(x) = \frac{\gamma' D}{4\mu K}\left(\exp\left(\frac{4\mu K}{D}x\right) - 1\right) \qquad (1)$$

where γ' is effective unit weight of the soil, μ the coefficient of friction between the pile and the soil, K the coefficient of the lateral pressure (ratio of lateral pressure to vertical pressure), and x is the distance from the top of the soil plug.

The results of the DEM analyses mentioned above are compared with the theoretical values below.

Figure 12 shows the relationships between H/D and the maximum push-up stress at the bottom of soil plug obtained from the theoretical equation (1) and the DEM analyses for the dense sand. The peak push-up stress in the DEM analysis is defined as the maximum value until the push-up displacement of 20 mm. The value of K in the theory was back-figured so as to get the agreement between the theoretical value and the DEM simulation result for each H/D.

It can be seen from Figure 12 that it is difficult to fit the theoretical result with the DEM simulation results for various H/D by employing a constant K irrespective of H/D. Similar result was obtained for the loose sand.

The back-calculated values of K are plotted in Figure 13 against H/D. It is seen from the figure that K-value tends to decrease with increasing H/D or increasing stress level in the soil plug. The decrease in K_0-value with increasing σ_v shown in Figure 5 corresponds to the decrease in K-value shown Figure 13, qualitatively. The K_0-value estimated from the oedometer test is much smaller than the back-calculated values of K in Figure 13. Therefore, the use of the equation proposed by Yamahara with K_0-value underestimates the soil plug capacity substantially, as indicated in Figure 12.

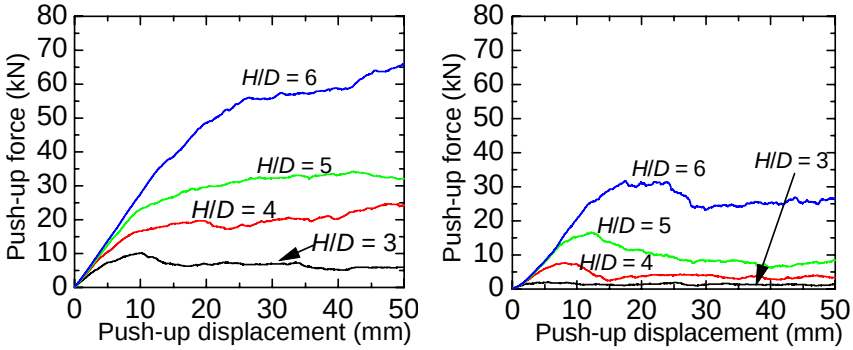

(a) Dense sand (clump) (b) Loose sand (sphere)

Figure 9. Relationships between push-up displacement and push-up force.

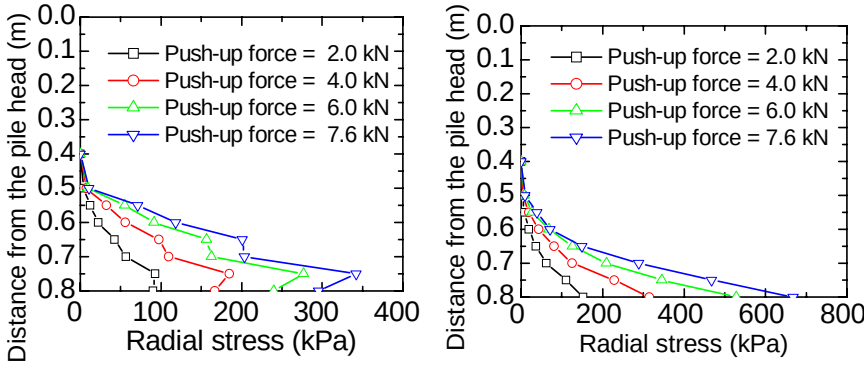

(a) Dense sand (clump) (b) Loose sand (sphere)

Figure 10. Distributions of radial stresses (for cases of H/D = 4).

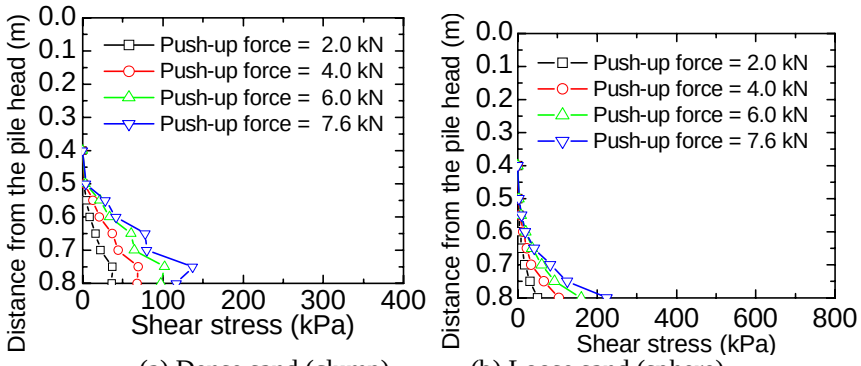

(a) Dense sand (clump) (b) Loose sand (sphere)

Figure 11. Distributions of shear stresses (for cases of H/D = 4).

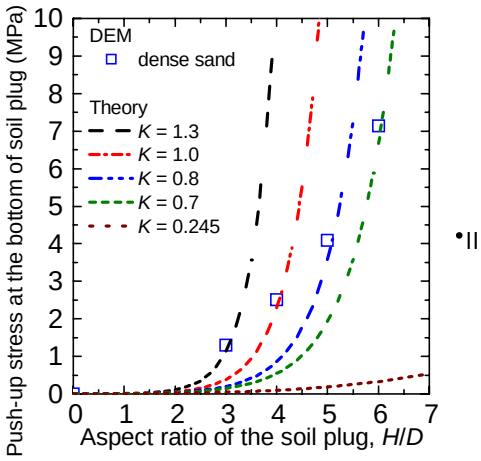

Figure 12. Comparison of peak push-up stresses from Yamahara's theory and DEM analyses for the dense sand.

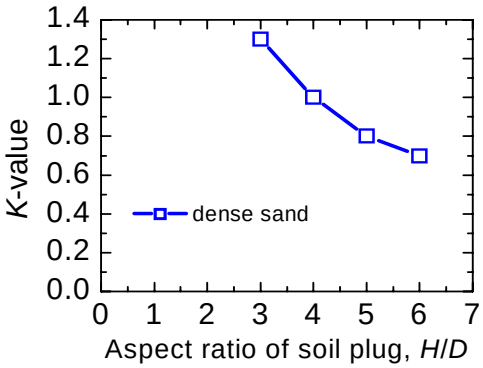

Figure 13. Back-calculated values of K.

4 CONCLUDING REMARKS

In this paper, parametric study on push-up loading of soil plug has been carried out using three-dimensional discrete element method (3D-DEM) to investigate the bearing mechanism of the soil plug.

Appropriate analysis parameters such as particle shape, coefficient of friction and spring stiffness between the particles were determined through the analyses of various element tests of the dense sand.

Parametric study on push-up loading was carried out using the determined parameters for different aspect ratios of the soil plug. Comparison of the analytical results with the theoretical equation by Yamahara was also made.

It was found through the analyses that aspect ratio of the soil plug and dilatancy behaviour of soil greatly affect the soil plug capacity in push-up loading, and that caution is needed when Yamahara's equation is employed to estimate the soil plug capacity.

REFERENCES

Itasca. 2003. PFC3D Manual, Itasca Corporation.

Japanese Geotechnical Society. 1992. Standards of Japanese Geotechnical Society for Laboratory Test (in Japanese).

Katzenbach, R. & Schmitt, A. 2004. Micromechanical modelling of granular materials under triaxial and oedometric loading. *Proc. 2nd Int. PFC Symp. on Numerical Modeling in Micromechanics via Particle Methods*: 313-322.

Kitiyodom, P., Matsumoto, T., Hayashi, M., Kawabata, N., Hashimoto, O., Ohtsuki, M. & Noji, M. 2004. Experiment on soil plugging of driven open-ended steel pipe piles in sand and its analysis. *Proc. 7th Int. Conf. on the Application of Stress-Wave Theory to Piles*: 447-458.

Matsumoto, T., Kitiyodom, P., Wakisaka, T. & Nishimura, S. 2004. Research on plugging of open-ended steel pipe piles and practice in Japan. *Proc. 7th Int. Conf. on the Application of Stress-Wave Theory to Piles*: 133-152.

Ovesen, N.K. 1979. Discussion 9.3 on 'The use of physical models in design,' *Proc. 7th European Conf. on SMFE*, Brighton, 4: 319-323.

Yamahara, H. 1964a. Plugging effects and bearing mechanism of steel pipe piles. *Trans. of the Architectural Inst. of Japan*, 96: 28-35 (in Japanese).

Yamahara, H. 1964b. Plugging effects and bearing mechanism of steel pipe piles (Part 2). *Trans. of the Architectural Inst. of Japan*, 97: 34-41 (in Japanese).